Journal of Earth and Planetary System Science
Volume 1, Issue 1, 31-51.
E-ISSN: 2963-1963
https://journal.gomit.id/jepss/index

Identification of Water Inundation-Prone Areas in Semarang Regency Using Landsat Frequency Analysis and Google Earth Engine (2020-2025)

Sofy Nabilah Balqis Eka Sugiarto*
Sekolah Tinggi Meteorologi Klimatologi dan Geofisika (STMKG), INDONESIA

*Sofy Nabilah Balqis Eka Sugiarto, Sekolah Tinggi Meteorologi Klimatologi dan Geofisika (STMKG), INDONESIA.
✉ cintasofy554@gmail.com

Article Info

Article history:

Received: July 25, 2026
Revised: Agustus 14, 2026
Accepted: Agustus 19, 2026

Keywords:
Google Earth Engine
Inundation frequency
Landsat
MNDWI
Water inundation

Abstract

Background: Water inundation is a recurring environmental hazard in Semarang Regency that frequently affects settlements, agricultural land, and infrastructure. Mapping inundation recurrence is essential for improving flood risk management and supporting spatial planning. The availability of cloud-based geospatial platforms such as Google Earth Engine (GEE) enables efficient multitemporal analysis of satellite imagery for monitoring inundation dynamics.
Aims: This study aims to identify and classify water inundation-prone areas in Semarang Regency by analyzing the spatial distribution and recurrence of inundation using Landsat observations acquired from 2020 to 2025.
Methods: Landsat 8 and Landsat 9 surface reflectance imagery, the administrative boundary of Semarang Regency, and SRTM Digital Elevation Model (DEM) data were processed in the Google Earth Engine environment. The Modified Normalized Difference Water Index (MNDWI) was calculated from the green and shortwave infrared bands to produce annual water masks. Pixel-based inundation frequency was summarized over six years and classified into vulnerability categories.
Results: Annual inundation extent fluctuated between 8.63 km^2 in 2020 and a maximum of 23.77 km^2 in 2021, before decreasing and increasing again to 15.16 km^2 in 2025. Recurrently inundated areas were mainly concentrated around Rawa Pening and surrounding lowlands characterized by flat to gently sloping terrain and dominated by agricultural and settlement land cover.
Conclusion: The proposed framework effectively integrates Landsat-derived MNDWI and Google Earth Engine to identify recurrent inundation patterns and produce spatially explicit vulnerability maps. The results provide valuable information for flood risk assessment, land-use planning, and disaster mitigation in Semarang Regency.

To cite this article: Sofy, N. B. E. S. (2026). Identification of Water Inundation-Prone Areas in Semarang Regency Using Landsat Frequency Analysis and Google Earth Engine (2020-2025). *Journal of Earth and Planetary System Science.* , *1*(1), 31-51.

INTRODUCTION

Water inundation remains a recurring hydrometeorological problem in many parts of Indonesia and has not been fully addressed. Inundation events are generally controlled by both natural and human-related factors, including high rainfall intensity, relatively flat terrain, land-use conversion, and limited drainage capacity. These conditions may disrupt community activities, damage infrastructure, reduce environmental quality, increase flood exposure, and cause economic losses (Merz et al., 2010; Tellman et al., 2021).

Semarang Regency in Central Java is one of the areas that is vulnerable to inundation. Its physiographic setting ranges from lowlands to hilly terrain, which influences surface runoff pathways and water accumulation. Rapid settlement growth and land conversion in recent years have also increased the potential for inundation, especially in low-slope areas with poor infiltration capacity. Therefore, Semarang Regency requires spatial identification and mitigation efforts for areas that are prone to water inundation (Badan Nasional Penanggulangan Bencana, 2025; Badan Penanggulangan Bencana Daerah Kabupaten Semarang, 2025; Pusat Krisis Kesehatan Kementerian Kesehatan Republik Indonesia, 2025; Badan Pusat Statistik Kabupaten Semarang, 2025).

Remote sensing has become an important approach in hydrological and disaster studies because it can provide spatially consistent observations over wide areas (Melesse et al., 2007; Huang et al., 2018). Landsat imagery is particularly useful for regional inundation analysis because it provides calibrated, multitemporal observations, a long global archive, and open data access at a spatial resolution suitable for regency-scale analysis (Roy et al., 2014; Wulder et al., 2019; Wulder et al., 2022; U.S. Geological Survey, 2025; Chander et al., 2009).

Inundation extraction from satellite imagery is commonly performed using spectral water indices. The Normalized Difference Water Index (NDWI) was introduced to enhance open-water features (McFeeters, 1996), while the Modified Normalized Difference Water Index (MNDWI) replaces the near-infrared band with shortwave infrared to improve water discrimination in built-up and mixed land-cover environments (Xu, 2006). Other water-extraction indices and threshold-based approaches have also been developed to reduce confusion from shadows, dark surfaces, mixed pixels, and local surface conditions (Feyisa et al., 2014; Ji et al., 2009; Huang et al., 2018). Multitemporal Landsat analysis has demonstrated the value of repeated observations for describing surface-water persistence and change (Pekel et al., 2016; Donchyts et al., 2016; Mueller et al., 2016).

Large-scale satellite processing requires adequate computational support. Google Earth Engine provides cloud-based access to global remote-sensing archives and high-performance geospatial processing (Gorelick et al., 2017; Kumar & Mutanga, 2018). Through this platform, Landsat images from 2020 to 2025 can be processed efficiently to examine the spatial and temporal frequency of inundation in Semarang Regency.

Inundation studies at the regency scale still require methods that describe repeated occurrence rather than only a single event. Satellite observations have become increasingly important for documenting flood exposure and inundation extent (Tellman et al., 2021), while optical and microwave flood-mapping research has emphasized the complementary strengths and limitations of different sensors (Schumann & Moller, 2015; Twele et al., 2016; Martinis et al., 2009; Markert et al., 2020; Kuenzer et al., 2013). Previous studies have also shown that terrain elevation, surface-water dynamics, and land-cover information can support the interpretation of flood-prone or inundation-prone environments (Farr et al., 2007; Yamazaki et al., 2017; Tarboton, 1997; Brown et al., 2022; Zanaga et al., 2021; Buchhorn et al., 2020). However, a pixel-based frequency approach can provide clearer information on locations that recur across multiple annual observations and may therefore deserve greater planning attention.

Inundation frequency analysis is important because it identifies locations with repeated surface-water occurrence and can complement event-based mapping (Pekel et al., 2016; Donchyts et al., 2016; Mueller et al., 2016; Tellman et al., 2021). The resulting information can support spatial planning, water-resource management, drainage improvement, and local disaster mitigation. Based on these needs, this study maps and classifies water inundation-prone areas in Semarang Regency using a six-year Landsat time series and Google Earth Engine (Gorelick et al., 2017; Kumar & Mutanga, 2018).

Based on these considerations, this study addresses three research questions: (1) how water inundation is spatially distributed in Semarang Regency based on Landsat imagery from 2020 to 2025; (2) how frequently inundation occurred during the observation period; and (3) which areas can be classified as prone to inundation based on frequency analysis.

The study aims to analyze the distribution of water inundation, calculate annual and multitemporal inundation frequency, and identify inundation-prone areas in Semarang Regency using Landsat imagery processed through Google Earth Engine.

METHOD

This study employed a descriptive quantitative research design based on remote sensing and spatial analysis to identify the spatial distribution, frequency, and vulnerability of water inundation in Semarang Regency. The study did not involve human participants or animals.

The analytical units were Landsat image pixels located within the administrative boundary of Semarang Regency, Central Java, Indonesia. The observation period covered 2020 to 2025, and the image dataset consisted of Landsat 8 and Landsat 9 scenes that met the temporal and image-quality criteria required for annual inundation analysis.

The primary data consisted of Landsat 8 and Landsat 9 imagery accessed and processed through Google Earth Engine (Roy et al., 2014; Wulder et al., 2019; Wulder et al., 2022; U.S. Geological Survey, 2025; Gorelick et al., 2017; Kumar & Mutanga, 2018). Administrative boundary data for Semarang Regency were used to define and clip the study area, while the 30 m Shuttle Radar Topography Mission Digital Elevation Model (SRTM DEM) supported slope derivation and topographic interpretation (Farr et al., 2007; Yamazaki et al., 2017). Land-cover information and historical flood records were used as supporting data for spatial interpretation and validation (Brown et al., 2022; Zanaga et al., 2021; Buchhorn et al., 2020).

Image preprocessing, spectral-index calculation, and spatial interpretation were conducted in Google Earth Engine following standard digital remote-sensing principles, including cloud masking, surface-reflectance processing, and large-scale geospatial analysis (Chander et al., 2009; Zhu & Woodcock, 2012; Gorelick et al., 2017; Kumar & Mutanga, 2018). The datasets, spatial or temporal resolutions, and analytical purposes used in this study are summarized in Table 1.

Table 1. Research Data and Data Sources

No	Data Type	Data Source	Resolution/Scale	Purpose
1	Landsat 8 and 9 imagery (2020-2025)	Google Earth Engine (USGS)	30 m, 16-day temporal resolution	Water-index analysis and inundation frequency mapping
2	Administrative boundary of Semarang Regency	Administrative boundary data	Regency scale	Study-area boundary and image clipping
3	Digital Elevation Model (DEM)	SRTM	30 m	Interpretation of topographic conditions

The research procedure consisted of several sequential stages. Landsat imagery from 2020 to 2025 was collected, selected, cloud-masked, filtered, and composited annually. Surface-water features were then extracted using the Modified Normalized Difference Water Index (MNDWI), calculated from the green and shortwave-infrared bands (Xu, 2006; Huang et al., 2018). The resulting index values were classified into inundated and non-inundated pixels to generate annual inundation maps, considering that water-index thresholds can vary with mixed pixels and local surface conditions (Ji et al., 2009; Huang et al., 2018). Inundation area was calculated from the classified pixel area and converted into square kilometres and hectares. The overall analytical workflow is presented in Figure 1.

For the multitemporal analysis, the six annual binary inundation maps were summed at the pixel level to determine how often each location was identified as inundated during the observation period. Occurrence values ranged from 0 to 6: 0 represented not inundated, while counts of 1, 2, 3, 4, 5, and 6 were interpreted as very rarely inundated, rarely inundated, occasionally inundated, frequently inundated, very frequently inundated, and permanent water, respectively. The frequency results were spatially compared with slope, average MNDWI, and land-cover characteristics (Farr et al., 2007; Yamazaki et al., 2017; Tarboton, 1997; Brown et al., 2022; Zanaga et al., 2021; Buchhorn et al., 2020). Areas with repeated inundation occurrences were then grouped into inundation-prone levels, and historical flood records were used as supporting information to assess the spatial consistency of the satellite-derived results (Badan Nasional Penanggulangan Bencana, 2025; Badan Penanggulangan Bencana Daerah Kabupaten Semarang, 2025; Pusat Krisis Kesehatan Kementerian Kesehatan Republik Indonesia, 2025).

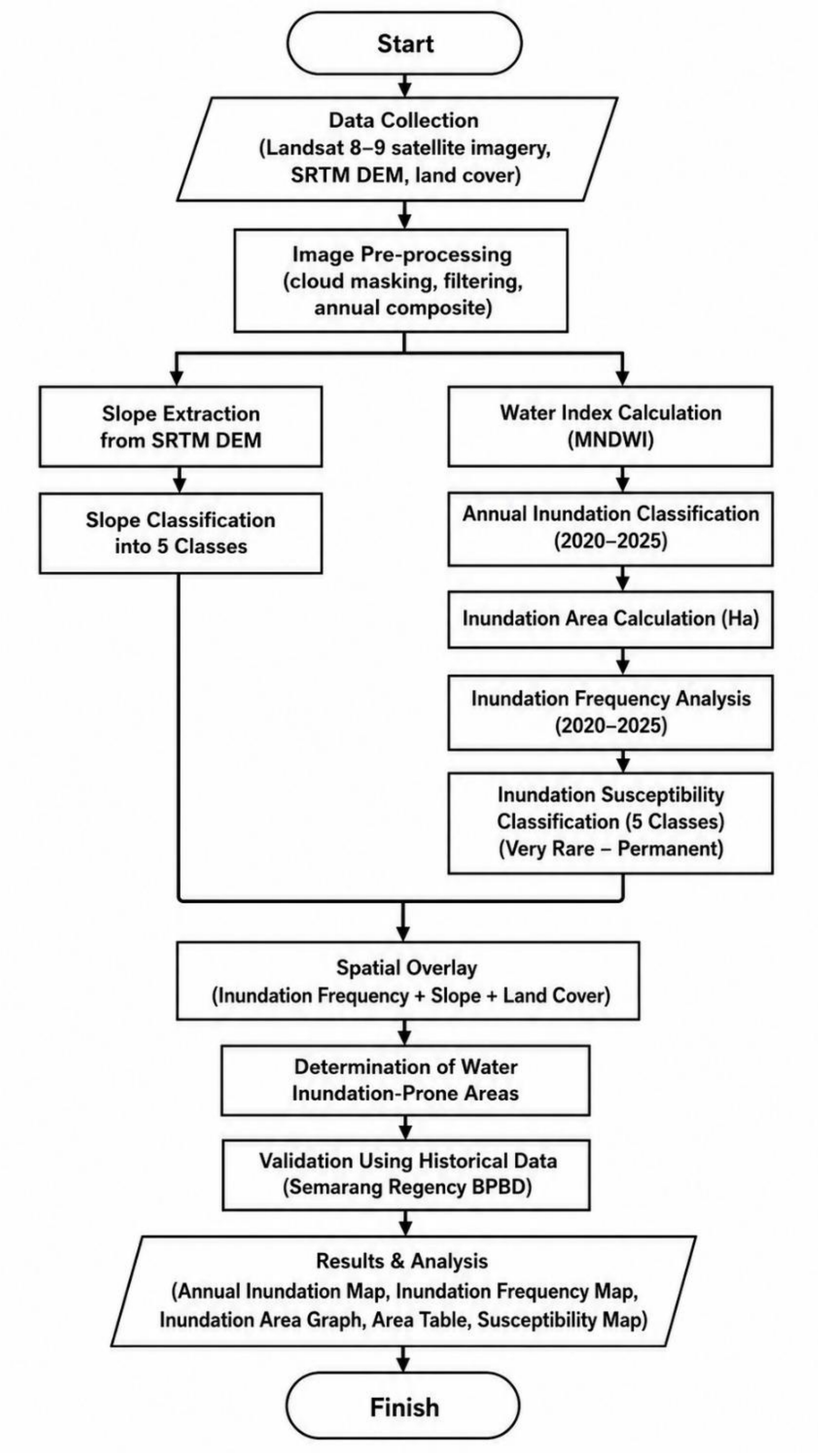

Figure 1. Research Workflow

The methodology was limited to Semarang Regency and the 2020-2025 observation period. The use of Landsat imagery at 30 m spatial resolution may limit the detection of small or narrow inundated features, and optical imagery may be affected by cloud availability and mixed pixels (Zhu & Woodcock, 2012; Ji et al., 2009; Huang et al., 2018). In addition, the annual-composite approach does not represent the exact duration or peak timing of individual inundation events. MNDWI-based classification may also capture permanent water bodies or water-related surface features. Historical flood records were therefore used only as supporting validation because complete field-based inundation observations with consistent spatial and temporal coverage were not available (Badan Nasional Penanggulangan Bencana, 2025; Badan Penanggulangan Bencana Daerah Kabupaten Semarang, 2025; Pusat Krisis Kesehatan Kementerian Kesehatan Republik Indonesia, 2025).

RESULTS AND DISCUSSION

3.1 Spatial Distribution of Water Inundation in Semarang Regency During 2020-2025

The spatial distribution of water inundation in Semarang Regency was obtained from annual Landsat classifications using MNDWI from 2020 to 2025 (Roy et al., 2014; Wulder et al., 2019; Wulder et al., 2022; U.S. Geological Survey, 2025; Xu, 2006; Huang et al., 2018). The maps show areas identified as inundated in each observation year, allowing the spatial pattern of inundation to be examined over time. The results indicate that inundation was not evenly distributed across the regency but tended to concentrate in specific locations.

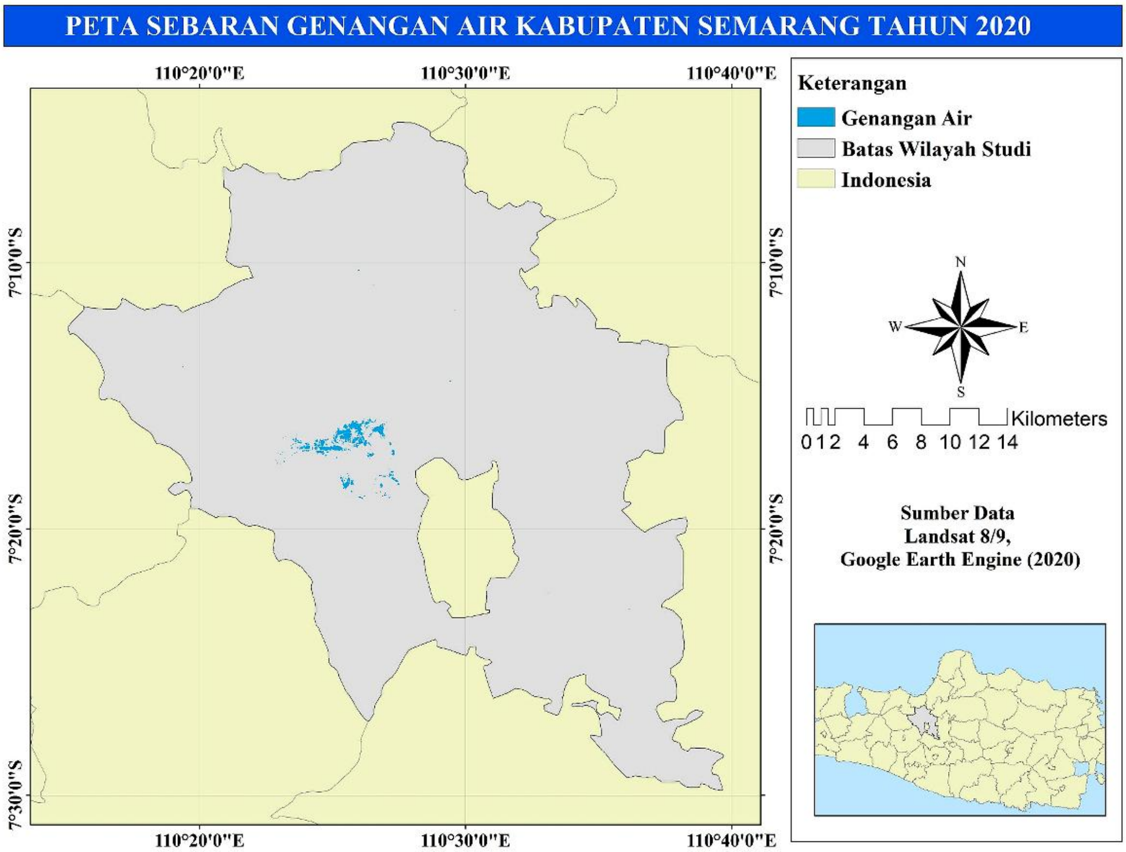

Figure 2. Water Inundation Distribution Map of Semarang Regency in 2020

Figure 2 shows that the identified inundation area in 2020 was relatively limited and appeared only in several localized sites. The distribution was fragmented and did not show extensive inundation, indicating that inundation during this year was mainly local in character.

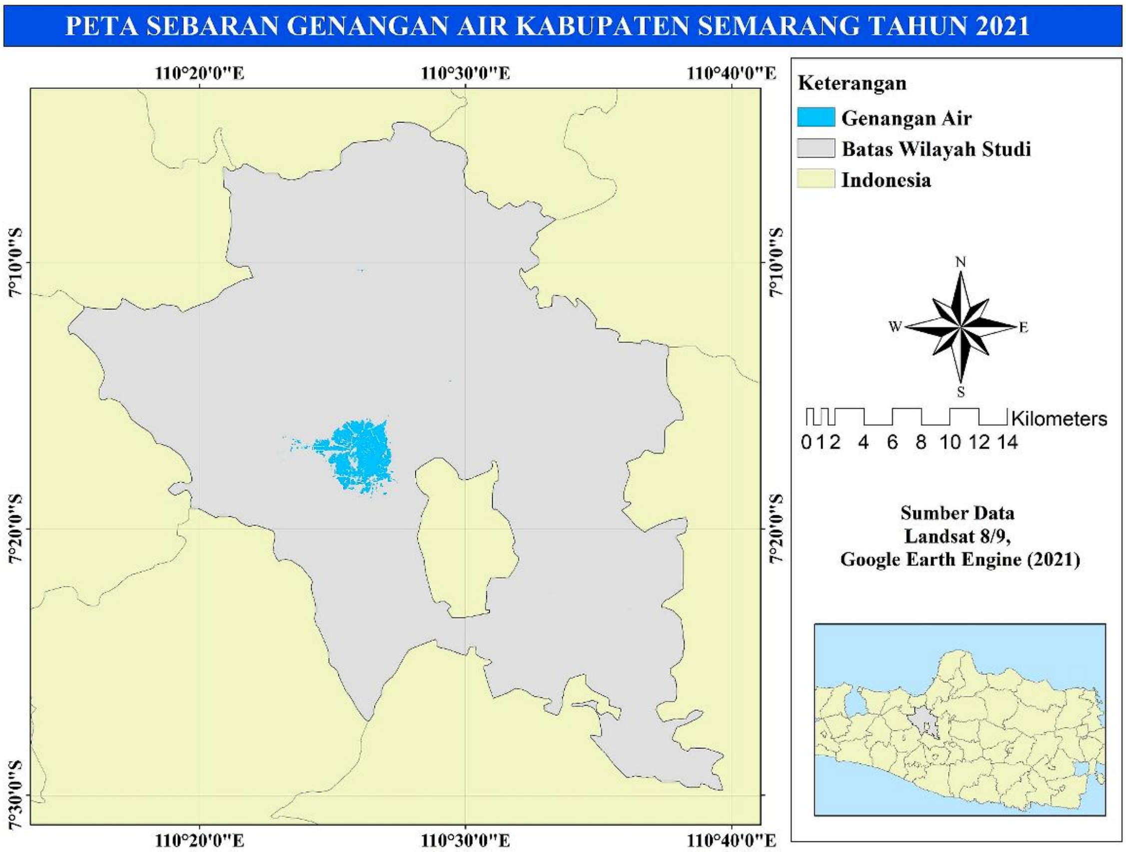

Figure 3. Water Inundation Distribution Map of Semarang Regency in 2021

Figure 3 shows that the inundation distribution increased in 2021 compared with the previous year. The inundated area became more concentrated and formed a main cluster in the central part of the study area, indicating stronger inundation occurrence in specific locations.

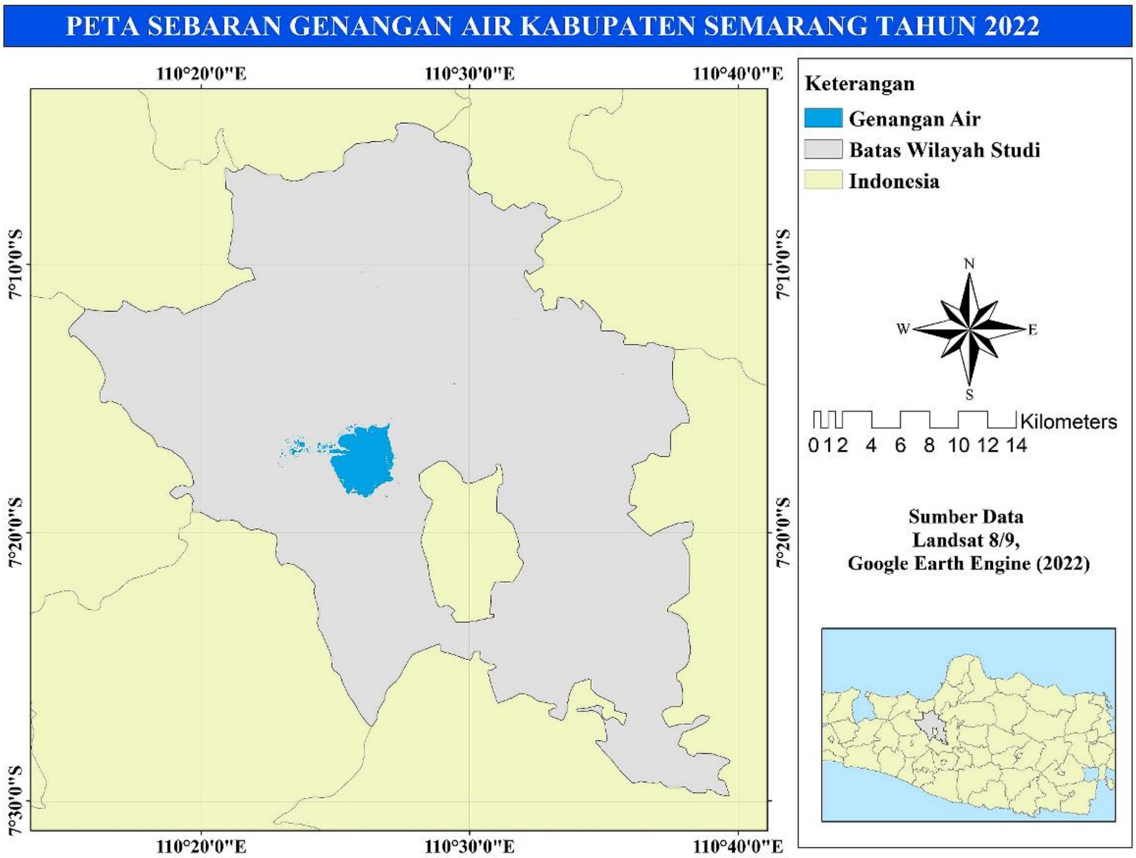

Figure 4. Water Inundation Distribution Map of Semarang Regency in 2022

Figure 4 shows that the 2022 inundation pattern was relatively similar to that of 2021, with a clearer inundation extent concentrated in the same area. This repeated occurrence suggests that some locations experienced recurring inundation.

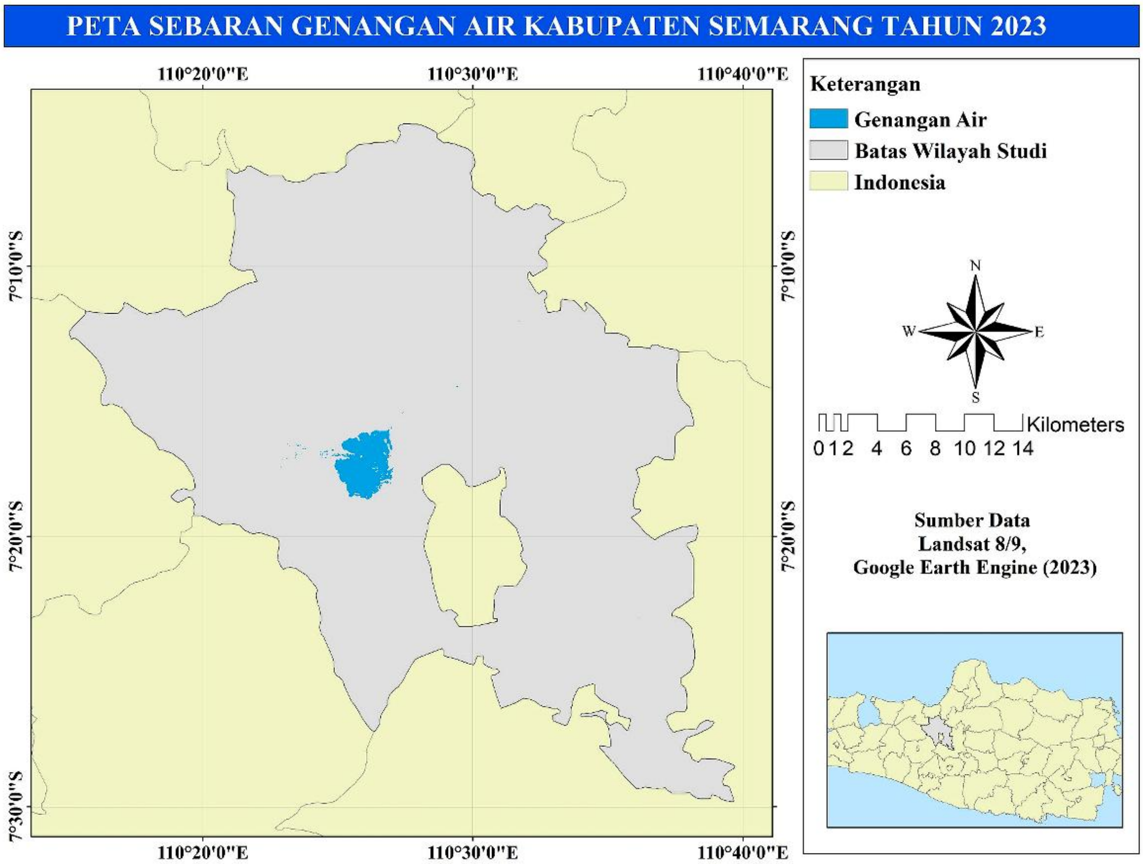

Figure 5. Water Inundation Distribution Map of Semarang Regency in 2023

Figure 5 shows that, in 2023, water inundation remained concentrated in the same general area, with a relatively stable extent compared with the previous year. This pattern indicates that the inundation location did not shift substantially and continued to occur in the same zone.

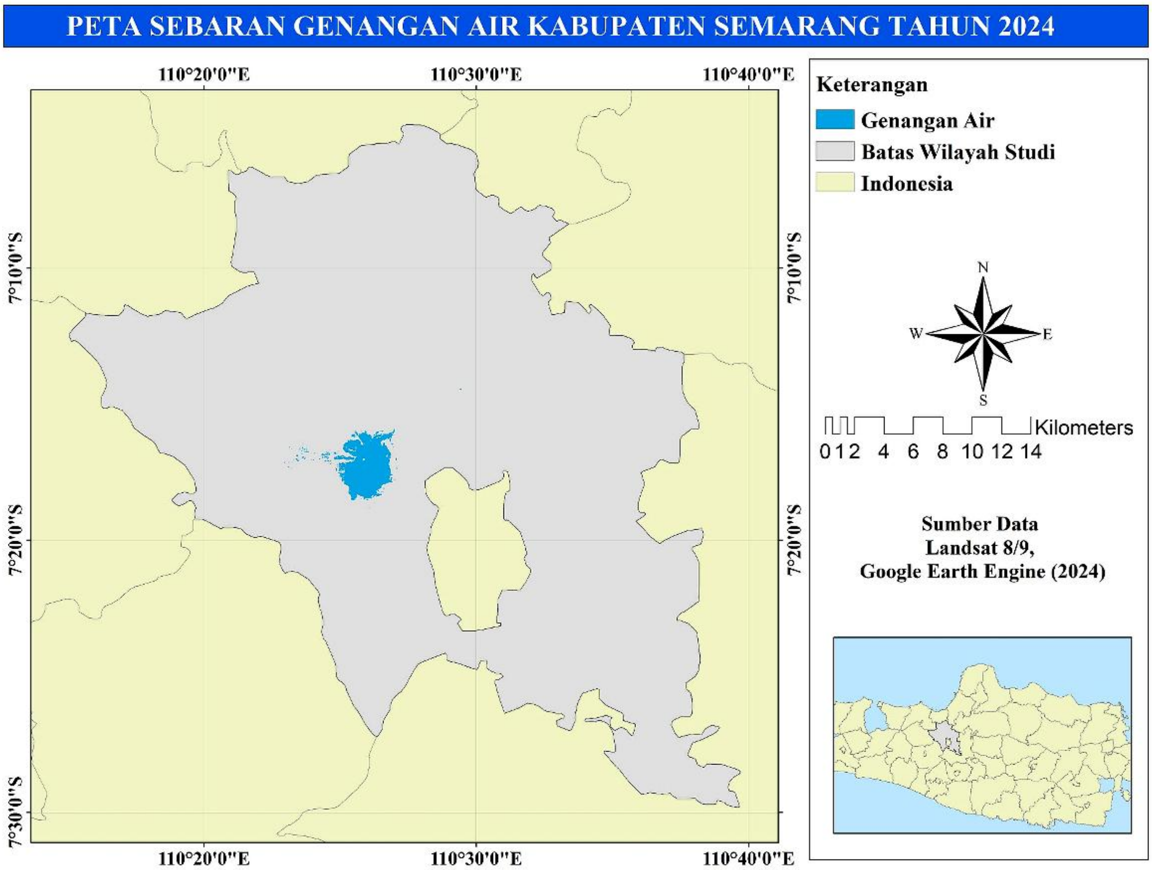

Figure 6. Water Inundation Distribution Map of Semarang Regency in 2024

Figure 6 shows an increase in inundation extent in 2024 within the main cluster in the central part of Semarang Regency. This indicates that inundation intensity in the area increased, although its spatial location remained broadly consistent.

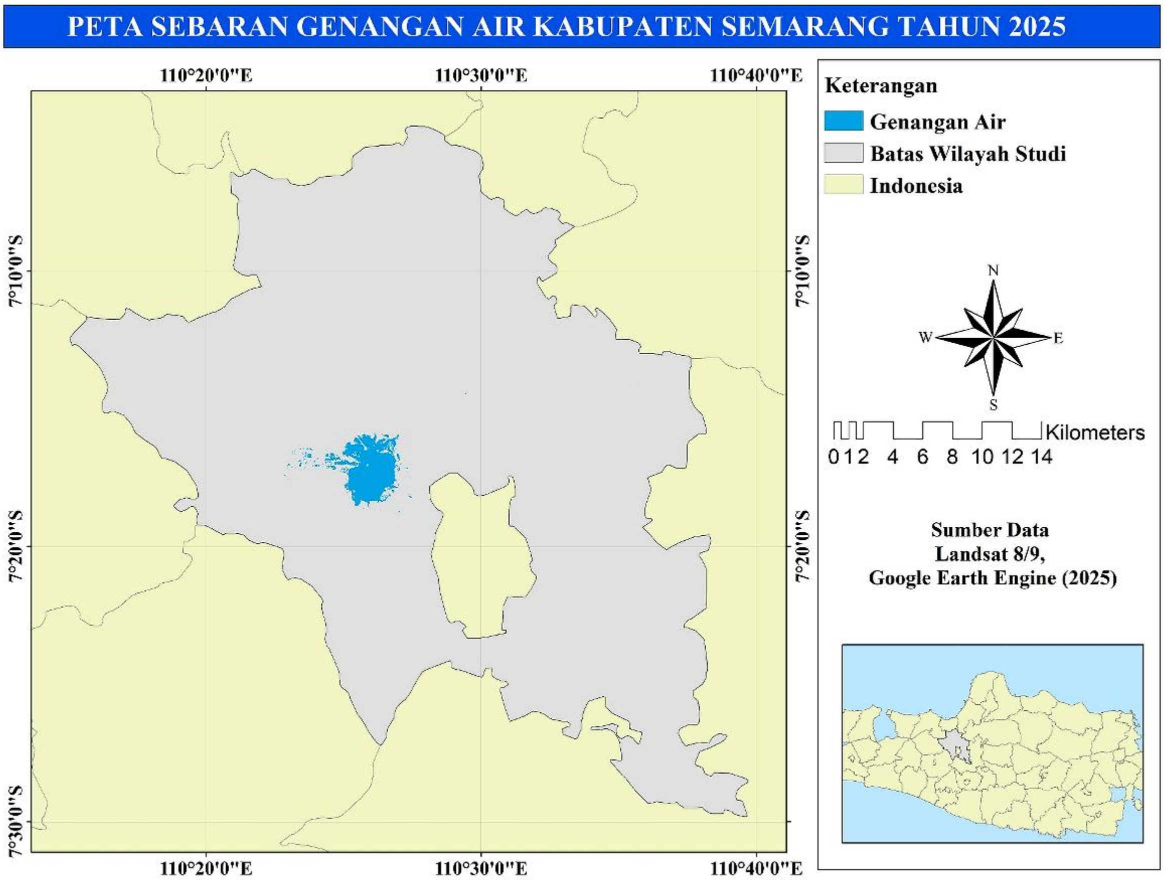

Figure 7. Water Inundation Distribution Map of Semarang Regency in 2025

Figure 7 shows that the 2025 inundation pattern remained spatially consistent with previous years. The repeated appearance of inundation in the same locations during 2020-2025 indicates the presence of areas with recurring inundation tendency, which became the basis for subsequent area and frequency analysis.

3.2 Inundation Area in Semarang Regency During 2020-2025

The inundation area in Semarang Regency was calculated from the annual Landsat-based inundation classifications. The number of inundated pixels was converted into area units, producing quantitative information on the inundated extent for each year from 2020 to 2025 (Roy et al., 2014; Wulder et al., 2019; Wulder et al., 2022; U.S. Geological Survey, 2025; Xu, 2006).

Table 2. Inundation Area in Semarang Regency during 2020-2025

Year	Area (km^2)	Area (ha)
2020	8.63	863
2021	23.77	2,377
2022	17.96	1,796
2023	13.08	1,308
2024	12.80	1,280
2025	15.16	1,516

Based on Table 2, the inundation area in Semarang Regency fluctuated during the observation period. The largest inundation area occurred in 2021, reaching 23.77 km^2 or approximately 2,377 ha, while the smallest occurred in 2020. After peaking in 2021, the inundation area generally decreased until 2024 and then increased again in 2025. This pattern shows that inundation was dynamic and varied from year to year.

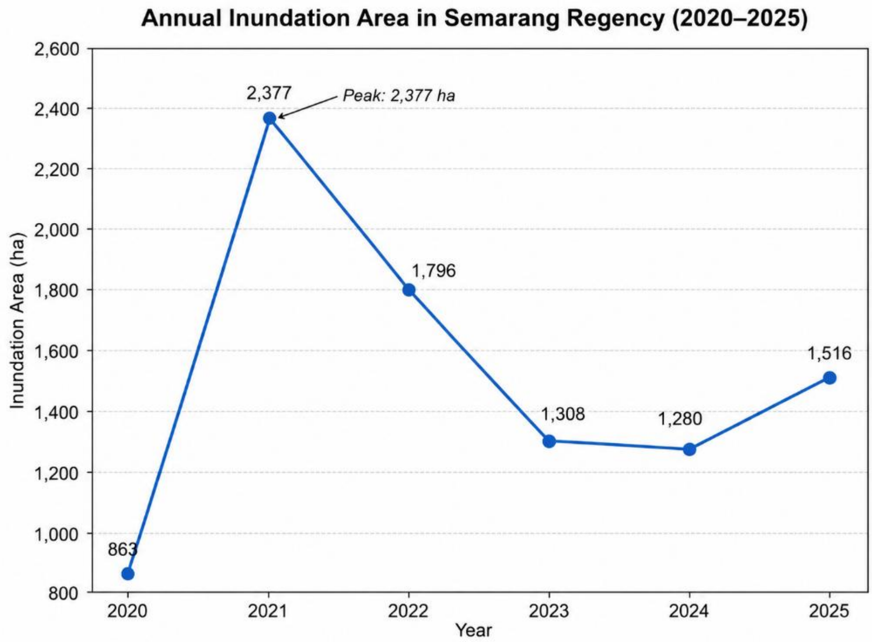

Figure 8. Graph of Inundation Area in Semarang Regency during 2020-2025

Figure 8 shows that annual changes in inundation area were not linear. Differences in inundation extent between years indicate that environmental conditions varied during the observation period. This area information is important for frequency analysis because annual variations help identify whether inundation was temporally dynamic and spatially concentrated during the observation period.

3.3 Inundation Frequency in Semarang Regency During 2020-2025

Inundation frequency was analyzed by combining annual inundation maps from 2020 to 2025 (Pekel et al., 2016; Donchyts et al., 2016; Mueller et al., 2016). This analysis was conducted to determine how often each location was identified as inundated during the six-year observation period. The frequency result represents the recurrence of inundation occurrence, not the final classification of inundation-prone areas. Each location was classified into several frequency categories, including not inundated, very rarely inundated, rarely inundated, occasionally inundated, frequently inundated, very frequently inundated, and permanent water.

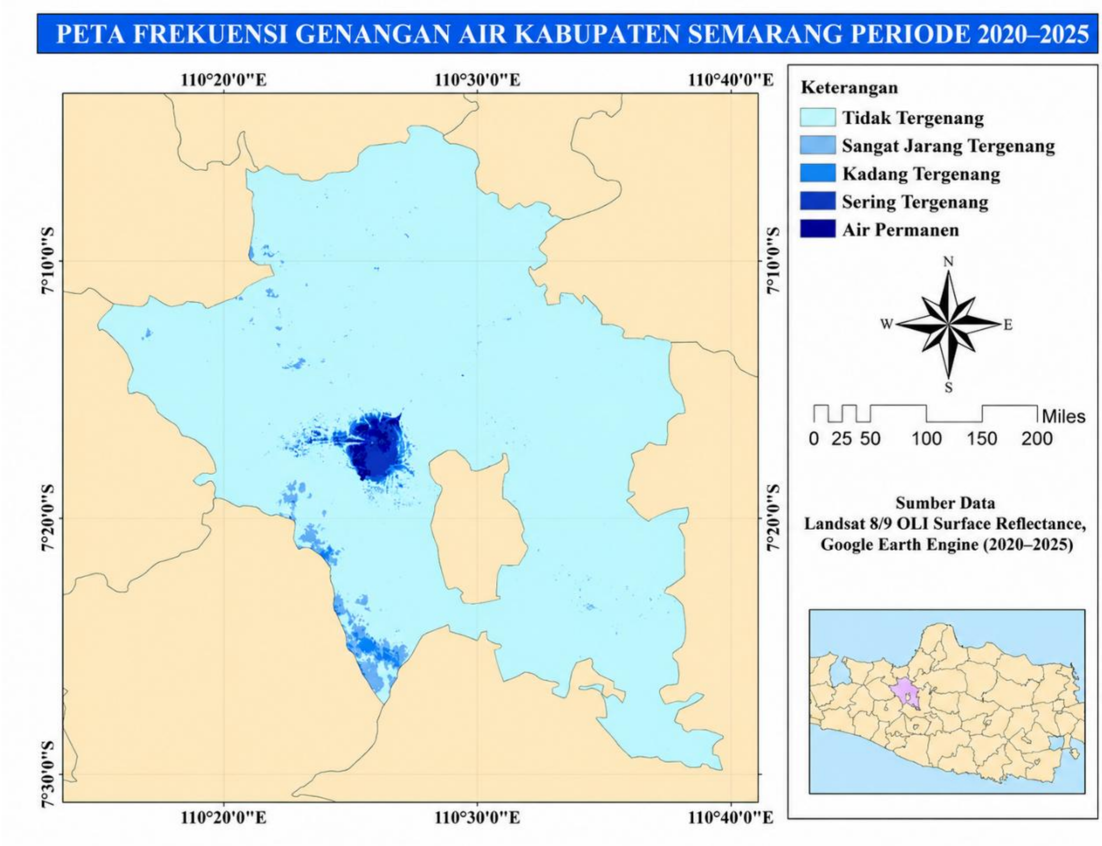

Figure 9. Inundation Frequency Map of Semarang Regency during 2020-2025

Figure 9 shows the spatial distribution of inundation frequency in Semarang Regency during 2020–2025. Most parts of the study area were classified as not inundated or very rarely inundated, indicating that repeated inundation did not occur across the entire regency. Higher-frequency classes were spatially concentrated in specific locations, particularly in the central part of the study area. This pattern indicates that inundation recurrence was localized rather than evenly distributed.

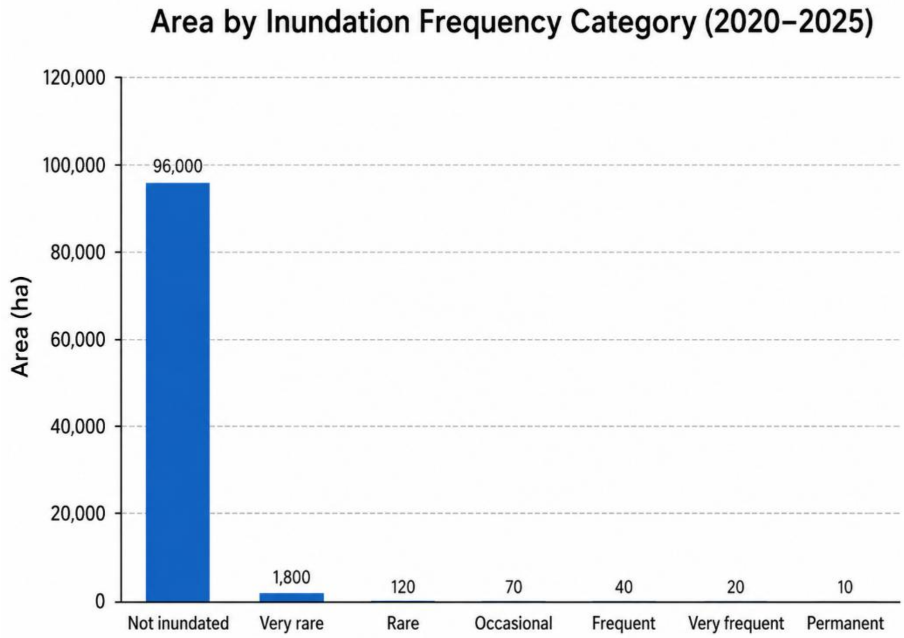

Figure 10. Graph of Inundation Area by Frequency Category during 2020-2025

Figure 10 shows that the not-inundated category occupied the largest area, while the inundated frequency categories covered much smaller extents. Among the inundated categories, the very rarely inundated class had the largest area, followed by rarely, occasionally, frequently, very frequently, and permanent-water classes. This result indicates that most inundation events were spatially limited, while repeated or persistent inundation occurred only in specific zones. Therefore, the frequency analysis provides an important basis for further interpretation of inundation-prone areas.

3.4 Relationship Between Inundation and Physical Characteristics of the Area

The frequency analysis indicates that inundation did not occur randomly but was concentrated in particular parts of Semarang Regency. This pattern suggests a relationship between inundation occurrence and physical land characteristics. To strengthen the interpretation, inundation patterns were compared with slope, average MNDWI values, and land cover (Farr et al., 2007; Yamazaki et al., 2017; Tarboton, 1997; Brown et al., 2022; Zanaga et al., 2021; Buchhorn et al., 2020).

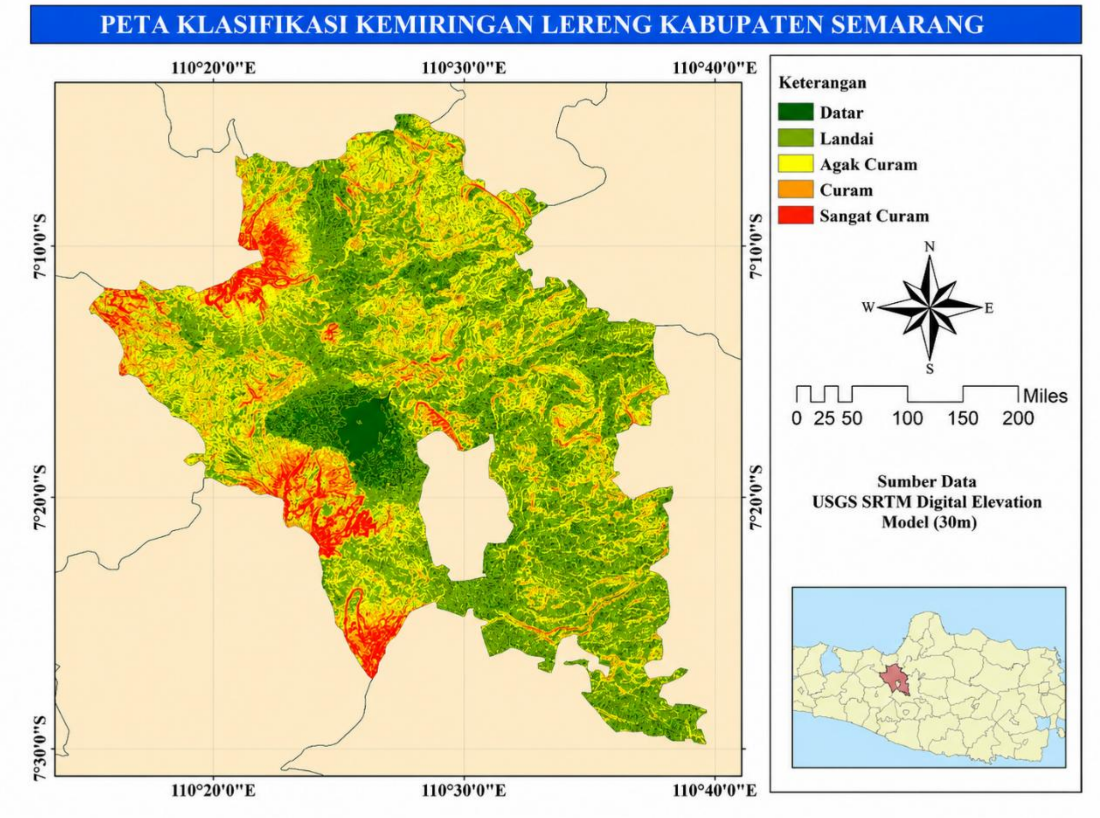

Figure 11. Slope Classification Map of Semarang Regency

Figure 11 shows that Semarang Regency consists of varied topography ranging from flat to very steep terrain. Inundated areas identified in the distribution and frequency maps tended to occur in flat to gently sloping areas. Low-slope areas generally have slower surface-water drainage, allowing water to accumulate and form inundation. In contrast, steep to very steep areas showed fewer inundation occurrences because water flows more rapidly downslope.

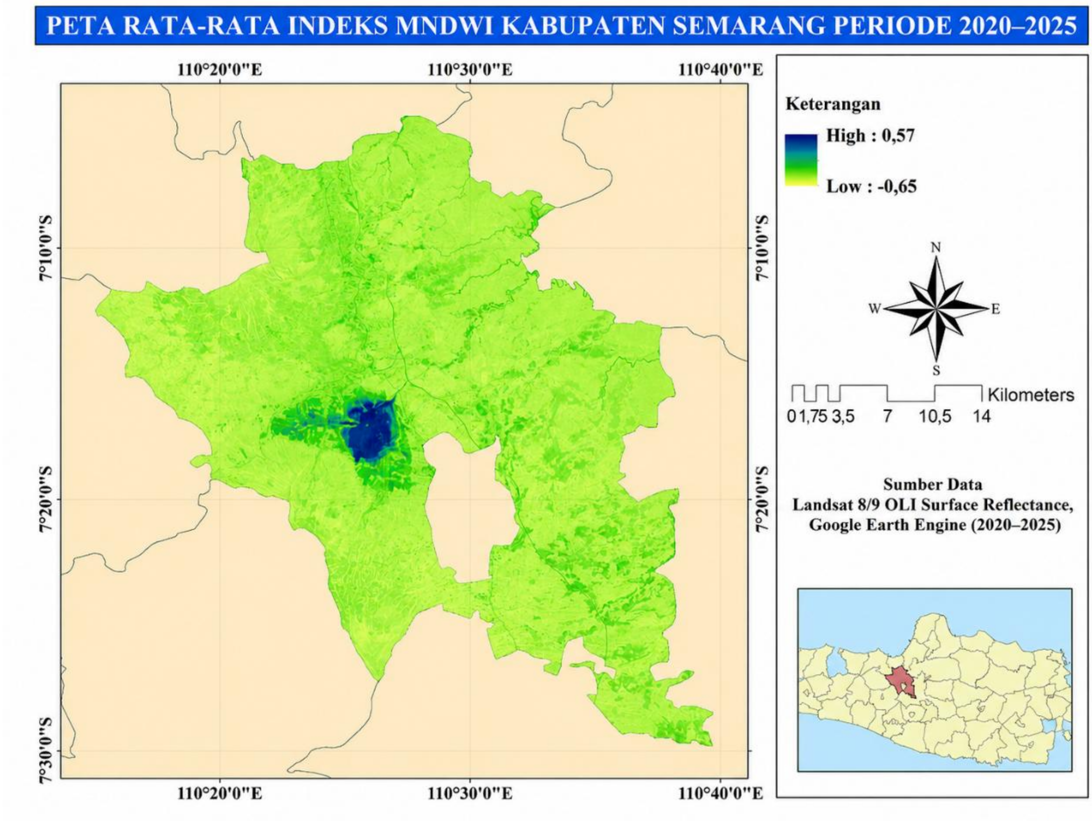

Figure 12. Average MNDWI Map of Semarang Regency during 2020-2025

Figure 12 shows that high average MNDWI values were concentrated in the same locations as the inundated areas identified in the distribution and frequency maps. High MNDWI values indicate surfaces with stronger water-related spectral response, supporting the inundation classification results. This spatial agreement is consistent with the intended behavior of MNDWI in enhancing open-water features and suppressing built-up, vegetation, and soil signals (Zhu & Woodcock, 2012).

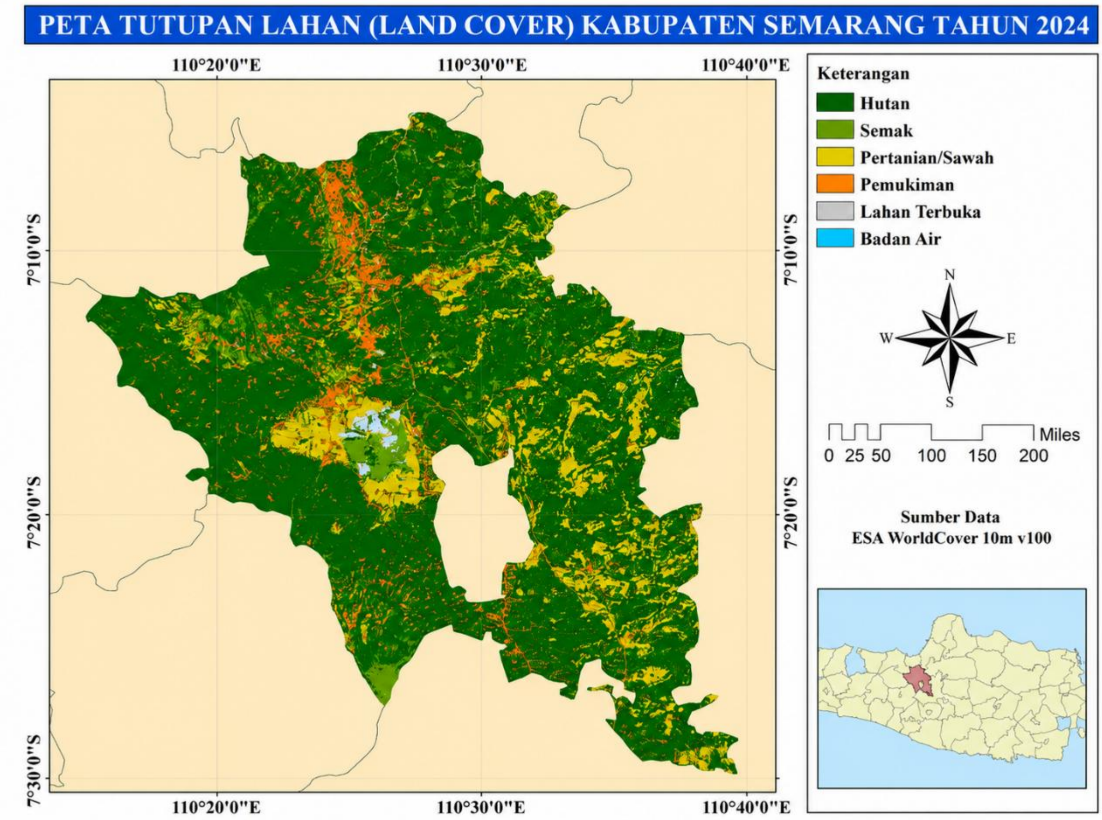

Figure 13. Land-Cover Map of Semarang Regency

Figure 13 shows that Semarang Regency is dominated by forest, agricultural or paddy fields, settlements, and open land. Inundated areas tended to occur in agricultural land, settlements, and open land. In the study area, the co-location of recurrent inundation with low-slope agricultural and settlement zones suggests that topography and land-cover conditions jointly influence where water accumulates. Similar Indonesian flood-mapping studies have reported the usefulness of combining satellite-derived water information with land-cover and terrain characteristics (Schumann & Moller, 2015; Twele et al., 2016; Kuenzer et al., 2013; Farr et al., 2007).

Based on these relationships, inundation events in Semarang Regency during 2020-2025 were influenced by the combination of topography, surface-water characteristics, and land-cover conditions. This interpretation became the basis for determining water inundation-prone areas in the next section.

3.5 Identification of Water Inundation-Prone Areas in Semarang Regency

Water inundation-prone areas in Semarang Regency were identified by interpreting the inundation frequency results together with the physical characteristics of the study area. The interpretation was mainly based on the recurrence of inundation during 2020-2025 and was supported by slope, average MNDWI, land-cover characteristics, and historical flood records (Farr et al., 2007; Yamazaki et al., 2017; Tarboton, 1997; Brown et al., 2022; Zanaga et al., 2021; Buchhorn et al., 2020; Badan Nasional Penanggulangan Bencana, 2025; Badan Penanggulangan Bencana Daerah Kabupaten Semarang, 2025; Pusat Krisis Kesehatan Kementerian Kesehatan Republik Indonesia, 2025; Badan Pusat Statistik Kabupaten Semarang, 2025). Therefore, this section presents the final interpretation of inundation-prone areas based on the results shown in the previous frequency and physical-characteristic analyses, rather than presenting a separate map with the same spatial output.

The results indicate that areas with higher inundation susceptibility were mainly concentrated in the central part of Semarang Regency, particularly around Rawa Pening and adjacent lowland areas. These locations showed repeated inundation occurrence, high water-related spectral response, flat to gently sloping terrain, and land-cover characteristics dominated by agricultural areas, settlements, or open land. Such conditions allow surface water to accumulate more easily and increase the possibility of recurring inundation.

Moderately prone areas were generally found in transition zones between lowland areas and areas with slightly higher slopes. These locations did not experience inundation as consistently as the high-prone zones, but they still showed inundation potential during the observation period. Meanwhile, low-prone areas were associated with locations that were rarely or very rarely identified as inundated. Areas with no inundation occurrence during 2020–2025 were not classified as inundation-prone areas.

Overall, the identification of water inundation-prone areas shows that inundation susceptibility in Semarang Regency is spatially concentrated rather than evenly distributed. The most important zones for mitigation are areas that repeatedly showed inundation occurrence and were supported by physical conditions that allow water accumulation. These results can support local planning, drainage improvement, and disaster-mitigation efforts, especially in areas around Rawa Pening and nearby lowland settlements.

3.6 Overall Discussion, Implications, and Study Limitations

Overall, the six-year results show that inundation in Semarang Regency was spatially persistent but temporally variable. The annual extent peaked in 2021 and did not follow a linear trend, while the frequency map identified a stable concentration of repeated water occurrence around Rawa Pening and adjacent lowlands. This distinction between annual extent and recurrence is important: a year with a large inundated area describes event magnitude at the annual-composite scale, whereas a high frequency value identifies pixels that repeatedly exhibit a water signal. The findings are consistent with the broader use of Landsat water indices and multitemporal surface-water mapping for inundation detection (McFeeters, 1996; Xu, 2006; Feyisa et al., 2014; Ji et al., 2009; Huang et al., 2018; Pekel et al., 2016; Donchyts et al., 2016; Mueller et al., 2016) and with studies that combine remote sensing, terrain, and land-cover information to interpret flood-prone environments (Schumann & Moller, 2015; Twele et al., 2016; Martinis et al., 2009; Markert et al., 2020; Kuenzer et al., 2013; Farr et al., 2007; Yamazaki et al., 2017; Tarboton, 1997; Brown et al., 2022; Zanaga et al., 2021; Buchhorn et al., 2020). The concentration of high-prone zones on flat to gently sloping land and in agricultural or settlement areas also supports the interpretation that local surface conditions influence water retention. However, the permanent-water class around Rawa Pening must be distinguished conceptually from episodic flooding: it represents persistent surface water in the six annual observations and serves as a hydrological context for nearby recurrent inundation rather than direct evidence that the lake itself is a flood impact zone.

The inundation-frequency map can be used as a first-level spatial screening product for Semarang Regency. High- and moderate-prone zones can be prioritized for drainage assessment, protection of water-retention pathways, control of land conversion in low-lying areas, and more detailed monitoring before and during the wet season. The results are especially relevant around Rawa Pening, where recurring water signals overlap with agricultural and settlement land cover.

The main contribution of this study is a simple and reproducible regency-scale framework that converts annual Landsat water masks into pixel-level inundation-occurrence classes. By integrating six annual observations with slope, land-cover interpretation, and historical-event comparison, the analysis moves beyond a single-event map and provides a spatial representation of recurrence that is directly interpretable for local planning.

This study has several limitations. The 30 m Landsat resolution may mix water and non-water features in narrow drainage channels, small ponds, and dense built-up areas. Optical observations are also constrained by cloud availability, and annual composites do not resolve event duration or peak timing. The study applied one consistent MNDWI classification rule, but threshold sensitivity and pixel-level classification accuracy were not evaluated using an independent field sample. Historical records were incomplete and therefore provided only supporting validation.

Future studies should calibrate and test the water-classification threshold with independent reference samples, integrate rainfall and river-network information, and compare annual Landsat results with higher-resolution or higher-frequency observations (Ji et al., 2009; Huang et al., 2018). Sentinel-1 SAR is particularly relevant for cloud-prone flood periods because microwave observations can support all-weather inundation mapping (Schumann & Moller, 2015; Twele et al., 2016; Martinis et al., 2009; Markert et al., 2020; Kuenzer et al., 2013). Sentinel-2 or finer DEM products may also improve delineation of narrow or heterogeneous inundation zones (Yamazaki et al., 2017; Tarboton, 1997; Brown et al., 2022; Zanaga et al., 2021; Buchhorn et al., 2020).

CONCLUSION

Landsat observations processed in Google Earth Engine showed that water inundation in Semarang Regency during 2020-2025 was unevenly distributed and tended to concentrate in specific recurrent zones. The annual inundation extent fluctuated from 8.63 km^2 (863 ha) in 2020 to a maximum of 23.77 km^2 (2,377 ha) in 2021, then decreased through 2024 before increasing again to 15.16 km^2 (1,516 ha) in 2025. Pixel-level frequency analysis indicated that most parts of the study area were classified as not inundated or very rarely inundated, while repeated water occurrence was concentrated around Rawa Pening and nearby lowland areas. The identified high-prone zones generally coincided with flat to gently sloping terrain and agricultural or settlement land cover. Comparison with available historical reports showed broad consistency with the 2021 flood period and renewed inundation conditions reported in 2025. Therefore, the six-year frequency framework provides a practical regional screening tool for spatial planning and inundation-risk mitigation, although further research should include field validation, rainfall and drainage data, and higher-resolution optical or SAR imagery to improve event discrimination and local-scale accuracy.

ACKNOWLEDGMENT

The author acknowledges the United States Geological Survey for Landsat data access, the providers of SRTM elevation data, and the public institutions whose historical flood information supported interpretation of the results. The author also acknowledges Sekolah Tinggi Meteorologi Klimatologi dan Geofisika (STMKG) as the author's academic institution.

USE OF ARTIFICIAL INTELLIGENCE (AI)-ASSISTED TECHNOLOGY

During the preparation of this work, the author used ChatGPT (OpenAI) to support English-language editing, manuscript organization, formatting adjustment, and figure presentation refinement in accordance with the journal template. After using this tool, the author reviewed, verified, and revised the manuscript as needed and takes full responsibility for the scientific content, data interpretation, and final version of the publication.

REFERENCES

Badan Nasional Penanggulangan Bencana. (2025). Data informasi bencana Indonesia (DIBI). https://dibi.bnpb.go.id

Badan Penanggulangan Bencana Daerah Kabupaten Semarang. (2025). Informasi kejadian bencana Kabupaten Semarang. https://bpbd.semarangkab.go.id

Badan Pusat Statistik Kabupaten Semarang. (2025). Kabupaten Semarang dalam angka 2025. https://semarangkab.bps.go.id

Brown, C. F., Brumby, S. P., Guzder-Williams, B., et al. (2022). Dynamic World, near real-time global 10 m land use land cover mapping. Scientific Data, 9, Article 251. https://doi.org/10.1038/s41597-022-01307-4

Buchhorn, M., Smets, B., Bertels, L., et al. (2020). Copernicus Global Land Service: Land cover 100 m: Collection 3: Epoch 2019: Globe. Remote Sensing, 12(6), Article 1044. https://doi.org/10.3390/rs12061044

Chander, G., Markham, B. L., & Helder, D. L. (2009). Summary of current radiometric calibration coefficients for Landsat MSS, TM, ETM+, and EO-1 ALI sensors. Remote Sensing of Environment, 113(5), 893–903. https://doi.org/10.1016/j.rse.2009.01.007

Cui, J., Guo, Y., Xu, Q., Li, D., Chen, W., Shi, L., Ji, G., & Li, L. (2023). Extraction of information on the flooding extent of agricultural land in Henan Province based on multi-source remote sensing images and Google Earth Engine. Agronomy, 13(2), Article 355. https://doi.org/10.3390/agronomy13020355

DeVries, B., Huang, C., Armston, J., Huang, W., Jones, J. W., & Lang, M. W. (2020). Rapid and robust monitoring of flood events using Sentinel-1 and Landsat data on the Google Earth Engine. Remote Sensing of Environment, 240, Article 111664. https://doi.org/10.1016/j.rse.2020.111664

Donchyts, G., Baart, F., Winsemius, H. C., Gorelick, N., Kwadijk, J., & van de Giesen, N. (2016). Earth's surface water change over the past 30 years. Nature Climate Change, 6(9), 810–813. https://doi.org/10.1038/nclimate3111

Farr, T. G., Rosen, P. A., Caro, E., et al. (2007). The Shuttle Radar Topography Mission. Reviews of Geophysics, 45(2), Article RG2004. https://doi.org/10.1029/2005RG000183

Fariz, T. R., Suhardono, S., Sultan, H., Rahmawati, D., & Arifah, E. Z. (2022). Land cover mapping in Lake Rawa Pening using Landsat 9 imagery and Google Earth Engine. Journal of Environmental and Science Education, 2(1), 1–6.

Feyisa, G. L., Meilby, H., Fensholt, R., & Proud, S. R. (2014). Automated Water Extraction Index: A new technique for surface water mapping using Landsat imagery. Remote Sensing of Environment, 140, 23–35. https://doi.org/10.1016/j.rse.2013.08.029

Gorelick, N., Hancher, M., Dixon, M., Ilyushchenko, S., Thau, D., & Moore, R. (2017). Google Earth Engine: Planetary-scale geospatial analysis for everyone. Remote Sensing of Environment, 202, 18–27. https://doi.org/10.1016/j.rse.2017.06.031

Hidayah, E., Pranadiarso, T., Halik, G., Indarto, I., Lee, W. K., & Maruf, M. F. (2022). Flood mapping based on open-source remote sensing data using an efficient band combination system. Acta Geographica Slovenica, 62(3), 47–62. https://doi.org/10.3986/AGS.10598

Huang, C., Chen, Y., Zhang, S., & Wu, J. (2018). Detecting, extracting, and monitoring surface water from space using optical sensors: A review. Reviews of Geophysics, 56(2), 333–360. https://doi.org/10.1029/2018RG000598

Ji, L., Zhang, L., & Wylie, B. (2009). Analysis of dynamic thresholds for the Normalized Difference Water Index. Photogrammetric Engineering & Remote Sensing, 75(11), 1307–1317. https://doi.org/10.14358/PERS.75.11.1307

Kuenzer, C., Guo, H., Huth, J., Leinenkugel, P., Li, X., & Dech, S. (2013). Flood mapping and flood dynamics of the Mekong Delta: ENVISAT-ASAR-WSM based time series analyses. Remote Sensing, 5(2), 687–715. https://doi.org/10.3390/rs5020687

Kumar, L., & Mutanga, O. (2018). Google Earth Engine applications since inception: Usage, trends, and potential. Remote Sensing, 10(10), Article 1509. https://doi.org/10.3390/rs10101509

Markert, K. N., Chishtie, F., Anderson, E. R., et al. (2020). Comparing Sentinel-1 surface water mapping algorithms and radiometric terrain correction processing in Southeast Asia utilizing Google Earth Engine. Remote Sensing, 12(15), Article 2469. https://doi.org/10.3390/rs12152469

Martinis, S., Twele, A., & Voigt, S. (2009). Towards operational near real-time flood detection using a split-based automatic thresholding procedure on high resolution TerraSAR-X data. Natural Hazards and Earth System Sciences, 9(2), 303–314. https://doi.org/10.5194/nhess-9-303-2009

McFeeters, S. K. (1996). The use of the Normalized Difference Water Index (NDWI) in the delineation of open water features. International Journal of Remote Sensing, 17(7), 1425–1432. https://doi.org/10.1080/01431169608948714

Mehmood, H., Conway, C., & Perera, D. (2021). Mapping of flood areas using Landsat with Google Earth Engine cloud platform. Atmosphere, 12(7), Article 866. https://doi.org/10.3390/atmos12070866

Melesse, A. M., Weng, Q., Thenkabail, P. S., & Senay, G. B. (2007). Remote sensing sensors and applications in environmental resources mapping and modelling. Sensors, 7(12), 3209–3241. https://doi.org/10.3390/s7123209

Merz, B., Kreibich, H., Schwarze, R., & Thieken, A. (2010). Assessment of economic flood damage. Natural Hazards and Earth System Sciences, 10(8), 1697–1724. 146 Review 2.docx

Mueller, N., Lewis, A., Roberts, D., et al. (2016). Water observations from space: Mapping surface water from 25 years of Landsat imagery across Australia. Remote Sensing of Environment, 174, 341–352. https://doi.org/10.1016/j.rse.2015.11.003

Pekel, J.-F., Cottam, A., Gorelick, N., & Belward, A. S. (2016). High-resolution mapping of global surface water and its long-term changes. Nature, 540(7633), 418–422. https://doi.org/10.1038/nature20584

Pusat Krisis Kesehatan Kementerian Kesehatan Republik Indonesia. (2025). Informasi kejadian krisis kesehatan akibat banjir. https://pusatkrisis.kemkes.go.id

Roy, D. P., Wulder, M. A., Loveland, T. R., et al. (2014). Landsat-8: Science and product vision for terrestrial global change research. Remote Sensing of Environment, 145, 154–172. https://doi.org/10.1016/j.rse.2014.02.001

Schumann, G. J.-P., & Moller, D. K. (2015). Microwave remote sensing of flood inundation. Physics and Chemistry of the Earth, Parts A/B/C, 83–84, 84–95. https://doi.org/10.1016/j.pce.2015.05.002

Sy, H. M., Luu, C., Bui, Q. D., Ha, H., & Nguyen, D. Q. (2023). Urban flood risk assessment using Sentinel-1 on the Google Earth Engine: A case study in Thai Nguyen city, Vietnam. Remote Sensing Applications: Society and Environment, 31, Article 100987. https://doi.org/10.1016/j.rsase.2023.100987

Tarboton, D. G. (1997). A new method for the determination of flow directions and upslope areas in grid digital elevation models. Water Resources Research, 33(2), 309–319. https://doi.org/10.1029/96WR03137

Tellman, B., Sullivan, J. A., Kuhn, C., et al. (2021). Satellite imaging reveals increased proportion of population exposed to floods. Nature, 596(7870), 80–86. https://doi.org/10.1038/s41586-021-03695-w

Twele, A., Cao, W., Plank, S., & Martinis, S. (2016). Sentinel-1-based flood mapping: A fully automated processing chain. International Journal of Remote Sensing, 37(13), 2990–3004. https://doi.org/10.1080/01431161.2016.1192304

U.S. Geological Survey. (2025). Landsat satellite missions. https://www.usgs.gov/landsat-missions/landsat-satellite-missions

Vanama, V. S. K., Mandal, D., & Rao, Y. S. (2020). GEE4FLOOD: Rapid mapping of flood areas using temporal Sentinel-1 SAR images with Google Earth Engine cloud platform. Journal of Applied Remote Sensing, 14(3), Article 034505. https://doi.org/10.1117/1.JRS.14.034505

Wulder, M. A., Loveland, T. R., Roy, D. P., et al. (2019). Current status of Landsat program, science, and applications. Remote Sensing of Environment, 225, 127–147. https://doi.org/10.1016/j.rse.2019.02.015

Wulder, M. A., Roy, D. P., Radeloff, V. C., et al. (2022). Fifty years of Landsat science and impacts. Remote Sensing of Environment, 280, Article 113195. https://doi.org/10.1016/j.rse.2022.113195

Xu, H. (2006). Modification of normalised difference water index (NDWI) to enhance open water features in remotely sensed imagery. International Journal of Remote Sensing, 27(14), 3025–3033. https://doi.org/10.1080/01431160600589179

Yamazaki, D., Ikeshima, D., Tawatari, R., et al. (2017). A high-accuracy map of global terrain elevations. Geophysical Research Letters, 44(11), 5844–5853. https://doi.org/10.1002/2017GL072874

Zanaga, M., Van De Kerchove, R., De Keersmaecker, W., et al. (2021). ESA WorldCover 10 m 2020 v100 [Data set]. Zenodo. https://doi.org/10.5281/zenodo.5571936

Zhu, Z., & Woodcock, C. E. (2012). Object-based cloud and cloud shadow detection in Landsat imagery. Remote Sensing of Environment, 118, 83–94. https://doi.org/10.1016/j.rse.2011.10.028